COMMUNICATION

Durable Transition-Metal-Carbide-Supported Pt–Ru Anodes for Direct Methanol Fuel Cells

K. G. Nishanth[1], P. Sridhar[1], S. Pitchumani[1], and A. K. Shukla[2]*

[1] CSIR-Central Electrochemical Research Institute, Madras Unit, CSIR Madras Complex, Chennai 600113, India
[2] Solid State and Structural Chemistry Unit, Indian Institute of Science, Bangalore 560012, India

Abstract

Molybdenum carbide (MoC) and tungsten carbide (WC) are synthesized by direct carbonization method. Pt–Ru catalysts supported on MoC, WC, and Vulcan XC-72R are prepared, and characterized by X-ray diffraction, X-ray photoelectron spectroscopy, and transmission electron microscopy in conjunction with electrochemistry. Electrochemical activities for the catalysts towards methanol electro-oxidation are studied by cyclic voltammetry. All the electro-catalysts are subjected to accelerated durability test (ADT). The electrochemical activity of carbide-supported electro-catalysts towards methanol electro-oxidation is found to be higher than carbon-supported catalysts before and after ADT. The study suggests that Pt–Ru/MoC and Pt–Ru/WC catalysts are more durable than Pt–Ru/C. Direct methanol fuel cells (DMFCs) with Pt–Ru/MoC and Pt–Ru/WC anodes also exhibit higher performance than the DMFC with Pt–Ru/C anode.

Keywords: DMFCs, Durability, Electro-catalyst, Methanol Electro-oxidation, Transition Metal Carbide

1 Introduction

Carbon-supported Pt–Ru (Pt–Ru/C) is the most effective catalyst for methanol electro-oxidation in direct methanol fuel cells (DMFCs) [1–4]. But the long-term stability of Pt–Ru electro-catalyst is a serious problem as Ru from the Pt–Ru anode tends to cross through the proton exchange membrane and deposit on to the Pt cathode affecting its performance [5]. Needless to add that ruthenium loss from Pt–Ru catalyst also degrades the catalytic activity of anode. Ru cations in the polymer electrolyte membrane affect its characteristic features, for example, an increase in the number of Ru ions per sulfonic acid group in the membrane decreases the water uptake of the membrane and increases the microviscosity of the fluidic regions possibly due to a change in the free volume of the membrane. Furthermore, Ru ions present in the membrane affect its proton conductivity, and accelerate membrane degradation [6–8]. Recently, the effects of catalyst-carbon support on proton conduction have been studied in detail by Liu et al. [9].

In the light of the foregoing, it is important to develop Pt–Ru catalyst supports with strong metal-to-support interaction so as to help preventing Ru metal dissolution to enhance the Pt–Ru catalyst stability in an operational DMFC. To this end, transition-metal carbides (TMCs) are an attractive option owing to their unique chemical and physical properties [10, 11]. The carbides of Groups IV–VI, in particular, exhibit catalytic properties akin to platinum-group metals. Indeed, there have been several attempts to utilize tungsten carbide (WC) as an electro-catalyst because of its platinum-like catalytic behavior, its stability in acid solutions at anodic potentials, and its resistance to CO poisoning [12]. But when used as an anodic material in a DMFC, pristine WC exhibits low electro-catalytic activity albeit its resistance to CO poisoning [13]. TMCs exhibit good mechanical and chemical stability and resistance against corrosion under operating conditions. TMCs also have several advantages over their parent metals in activity, selectivity, and resistance to poisoning.

In the present study, an attempt is therefore made to enhance the catalytic activity and durability of Pt–Ru alloy catalyst by supporting it on to molybdenum and WC. Molyb-

---

denum carbide (MoC) and WC are prepared by direct carbonization method and Pt–Ru is supported on them by chemical impregnation using NaBH$_4$ as reducing agent. The crystalline nature and alloy formation in Pt–Ru/MoC and Pt–Ru/WC catalysts are confirmed by powder X-ray diffraction (XRD), their chemical nature is studied by X-ray photoelectron spectroscopy (XPS) and their morphologies are examined by transmission electron microscopy (TEM). Methanol electrooxidation and accelerated durability test (ADT) are performed on Pt–Ru/C, Pt–Ru/MoC, and Pt–Ru/WC catalysts using cyclic voltammetry (CV). DMFCs with Pt–Ru/MoC, Pt–Ru/WC, and Pt–Ru/C anodes have also been performance tested and it is found that DMFCs with carbide-supported Pt–Ru anodes exhibit higher performance in relation to the DMFC with carbon-supported Pt–Ru anode. It is strongly believed that the findings reported in the study would help furthering the performance and stability of Pt–Ru catalyst in DMFCs.

2 Experimental

2.1 Materials

Sodium tungstate hydrate (Na$_2$WO$_4$·2H$_2$O) and sodium molybdate hydrate (Na$_2$MO$_4$·2H$_2$O) were purchased from SRL Private Ltd., India. Hydroxy propyl cellulose (HPC) was obtained from Acros Organics, and polyvinyl alcohol (PVA) was procured from Loba Chemie Private Ltd., India. Dihydrogen hexachloroplatinate (IV) hexahyrate (H$_2$PtCl$_6$·6H$_2$O) was purchased from Alfa Aesar (Johnson Matthey) Chemicals. Ruthenium (III) chloride hydrate was obtained from Acros Organics. Sodium borohydride (NaBH$_4$) was procured from S. D. Fine-Chem. Toray TGP-H-120 carbon paper was procured from Nikunj Exim Pvt. Ltd., India. Vulcan XC-72R carbon was obtained from Cabot. Poly-tetrafluoroethylene (PTFE) emulsion was procured from Hindustan Fluorocarbons Ltd., India. 5% Nafion ionomer was procured from DuPont, US. Pt/C (40 wt.% Pt on Vulcan XC-72R carbon) was procured from Johnson Matthey Chemicals India Pvt. Ltd. 2-Propanol and methanol, and perchloric acid (HClO$_4$) and sulfuric acid (H$_2$SO$_4$) were procured from Merck-India and Rankem-India, respectively. Deionized (DI) water (conductivity 18.4 MΩ cm) from a Millipore system was used during the experiments.

2.2 Preparation of Tungsten and Molybdenum Carbides

The starting materials used were HPC and PVA as carbon precursors while Na$_2$WO$_4$ and Na$_2$MoO$_4$, reagent grade were employed as precursors for tungsten and MoCs, respectively [14, 15]. 0.5 g of Na$_2$WO$_4$ (or Na$_2$MoO$_4$) was dissolved in 25 mL of DI water followed by addition of 75 mL of ethanol. Subsequently, a mixture of 2 g HPC and 2 g PVA was slowly added to it under vigorous stirring. A gel obtained after ~2 h was dried at 100 °C for 24 h. Subsequently, carbonization was performed by heating to 900 °C at a heating rate of

5 °C min^{-1} under flowing nitrogen (200 mL min^{-1}) for 3 h. After the heat-treatment, the solid was ground, washed with 1 M aq. H$_2$SO$_4$ followed with copious washing with distilled water and subsequent drying in an air-oven.

2.3 Preparation of Supported Pt–Ru

Thirty wt.% Pt–Ru (1:1) supported on WC, MoC, or Vulcan XC-72R carbon black were prepared as follows. In brief, the support was suspended in DI water and subjected to ultrasonication for 20 min, and to the resulting ink the solutions of chloride precursors of Pt and Ru were added followed with mixing for 15 min. The pH value of the resultant mixture was adjusted to 9 using NaOH solution. Subsequently, the temperature was raised to 80 °C followed by addition of NaBH$_4$ solution. After 45 min, the prepared catalysts were filtered and washed with hot DI water and dried. The supported catalyst powders were heat-treated with a gaseous mixture containing N$_2$ and H$_2$ in 9:1 ratio at 300 °C in a tubular furnace for 5 h to obtain the supported Pt–Ru alloy catalysts.

2.4 Physical Characterization of the Catalysts

The crystalline structure of the supported catalysts were studied by recording their X-ray powder diffraction patterns between 20 and 90° in reflection geometry in steps of 5° min^{-1} using Cu Ka radiation (λ = 1.5406 Å). X-ray photoelectron spectra for the various catalysts were recorded on a VG Micro-Tech ESCA 300° instrument at a pressure >10^{-9} Torr and pass energy of 50 eV with electron take-off angle of 60° and overall resolution of ~0.1 eV. The structure and morphology of electro-catalysts were characterized using a TEM (JEOL model 1200 EX) operating at an accelerating voltage of 120 kV.

2.5 Electrochemical Measurements

Electrochemical measurements were performed with an electrochemical analyzer (Autolab PGSTAT-30), using a conventional 3-electrode test cell with a saturated calomel electrode (SCE) and a platinum foil as the reference and counter electrodes, respectively. The glassy carbon working electrodes (0.071 cm^2) were prepared as follows: 10 mg of supported catalyst, 10 wt.% of Nafion solution (DuPont, USA) and 3 mL of ultra pure water were mixed ultrasonically, and 20 μL of the suspension was quantitatively transferred to the surface of the freshly polished-glassy-carbon disk. The electrode was dried at room temperature. Prior to any electrochemical measurement, the working electrode was cycled between 0.25 and 0.8 V versus SCE at a sweep rate of 50 mV s^{-1}. Experiments were conducted in nitrogen-purged 0.5 M aq. HClO$_4$ solution for removing any contaminant from the electrode and activating it. ADT on electro-catalysts were carried out in a solution containing aq. 0.5 M HClO$_4$ and aq. 0.5 M CH$_3$OH in the potential range between 0.36 and 0.86 V versus SCE at a scan rate of 10 mV s^{-1} for 1,000 cycles. CVs

were recorded in the potential range –0.23 and 1 V *versus* SCE at a scan rate of 50 mV s^{-1}. All experiments were carried out at 25 °C. The amount of Ru leached out during ADT from the catalysts was estimated by ICP-MS analysis. The actual compositions were established from the calibration curves for the known standards.

2.6 Preparation of Membrane Electrode Assemblies and Their Performance Testing

The catalysts were evaluated in DMFCs by making membrane electrode assemblies (MEAs) following the procedure described elsewhere [16]. The loadings of Pt and Nafion in supported Pt–Ru alloy anode catalyst were kept at 1 mg Pt cm^{-2} and 10 wt.%, respectively, while that in the cathode catalyst were kept at 2 mg Pt cm^{-2} and 30 wt.%, respectively. The geometrical area of all the MEAs used in the present study was 4 cm^2. MEAs were performance tested using a conventional fuel cell fixture with a parallel serpentine flow-field machined on graphite plates (Schunk Kohlenstofftechnic). The cells were performance tested at 70 °C with 2 M aq. methanol at a flow rate of 2 sccm at the anode side while the flow rate of oxygen at 200 sccm at the cathode side. The galvanostatic polarization data were recorded using an LCN100-36 electronic load procured from Bitrode Corporation, US. The reproducibility of the data was ascertained.

3 Results and Discussion

X-ray diffraction data shown in Figure 1(a) confirm the presence of the active crystalline phases for molybdenum and WCs. The hexagonal close packed (hcp) MoC and β-Mo$_2$C are
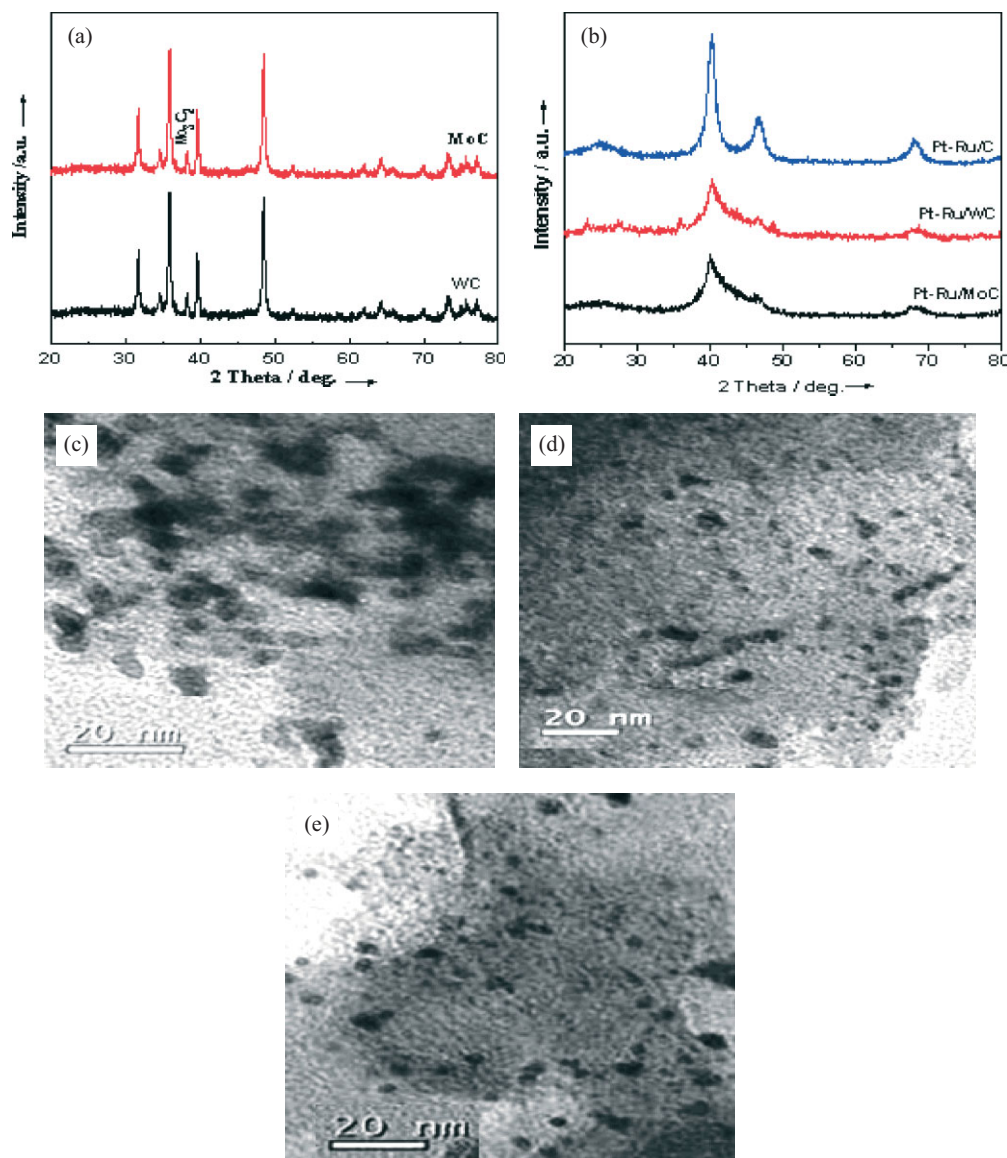

Fig. 1 Powder XRD patterns of (a) MoC, WC and (b) Pt–Ru/C, Pt–Ru/MoC and Pt–Ru/WC and transmission electron micrographs for (c) Pt–Ru/WC, (d) Pt–Ru/MoC, and (e) Pt–Ru/C catalysts.

clearly observed. Similar results are obtained for hcp WC and W_2C as shown in Figure 1(a) [14, 15].

Analysis of the powder XRD data for catalysts presented in Figure 1(b) reveals that Pt–Ru/C, Pt–Ru/MoC, and Pt–Ru/WC have a face-centered cubic (fcc) crystal structure. The average crystallite sizes calculated for Pt–Ru/WC, Pt–Ru/MoC, and Pt–Ru/C from the respective powder XRD patterns

by using Scherrer equation are 6.5, 5.6, and 7 nm, respectively. It is seen that carbide-supported catalysts exhibit slight shift in peak values to the lower angles relative to carbon-supported catalyst. For example, 2θ values corresponding to (111) plane are 40.3, 39.9, and 40.2° for Pt–Ru/C, Pt–Ru/MoC, and Pt–Ru/WC catalysts, respectively. This shift in 2θ values has been attributed to metal–support interaction [17].
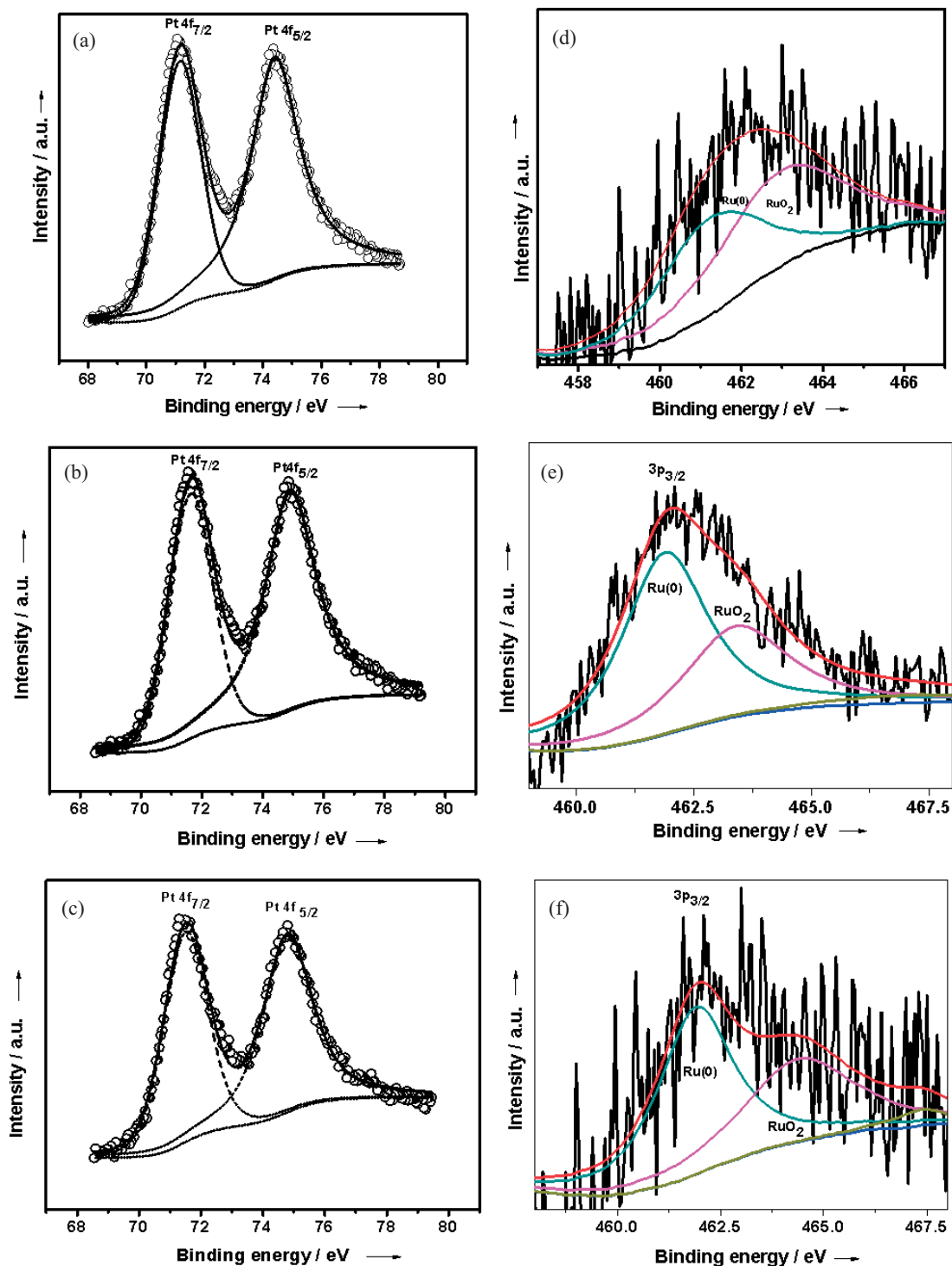

Fig. 2 Pt (4f) X-ray photoelectron spectra for (a) Pt–Ru/C, (b) Pt–Ru/MoC, and (c) Pt–Ru/WC, and Ru(3p) X-ray photoelectron spectra for (d) Pt–Ru/C, (e) Pt–Ru/MoC, and (f) Pt–Ru/WC.

Figure 1(c) shows the transmission electron micrograph for Pt–Ru/WC catalyst. A closer examination of the TEM image reveals that the alloy particles in the supported catalyst are randomly dispersed, while some of them aggregate to form larger particles typical of a cluster. The particle size is found to be in the range 5–9 nm. By contrast, the transmission electron micrograph for Pt–Ru/MoC shown in Figure 1(d) exhibits a uniform dispersion of the alloy particles on the carbide surface with particle size ranging between 4 and 8 nm. Figure 1(e) for Pt–Ru/Vulcan XC 72R also reveals dispersion of alloy particles on the carbon surface with particle ranging between 5 and 9 nm.

X-ray photoelectron spectroscopy is used to determine the surface oxidation state of the carbide supported catalysts. X-ray photoelectron spectra for Pt (4f) core level region in, Pt–Ru/MoC and Pt–Ru/WC catalysts are presented in Figure 2 (a–c). The spectra for Pt–Ru/C, Pt–Ru/MoC, and Pt–Ru/WC can be fitted into two sets of spin-orbit doublets. For Pt–Ru/C, the doublet at 71.15 and 74.41 eV in its Pt ($4f_{7/2,5/2}$) X-ray photoelectron spectrum is assigned to Pt^0 species. XPS data confirm the alloy formation with the binding energy for Pt^0 species in good agreement with Pt–Ru alloy [18]. For Pt–Ru/MoC, the Pt ($4f_{7/2,5/2}$) doublet at 71.68 and 74.91 eV is assigned to Pt^0. Similarly, Pt ($4f_{7/2,5/2}$) doublet in Pt–Ru/WC at 71.50 and 74.86 eV is assigned to Pt^0. It is noteworthy that in all the catalysts, Pt is devoid of any metallic oxides and is present only in the metallic state. It could be due to the heat treatment with a gaseous mixture containing N_2 and H_2 in 9:1 ratio at 300 °C for 5 h, which facilitates the complete conversion of oxidized Pt to Pt^0 state. The shift to higher binding energy values in Pt ($4f_{7/2,5/2}$) doublets for Pt^0 species in Pt–Ru/MoC and Pt–Ru/WC from the standard Pt($4f_{7/2,5/2}$) doublet at 71.15 and 74.41 eV due to Pt^0 species in Pt–Ru/C may be attributed to the interaction between catalyst metals and carbide supports and/or to the small cluster size effect [18, 19]. Ru (3p) spectra have been analyzed here instead of Ru (3d) spectra because the latter overlaps with C (1s) spectra as shown in Figure 2(d–f). Ru ($3p_{3/2}$) spectrum for Pt–Ru/C can be deconvoluted into two distinct peaks at 461.4 and 463.4 eV corresponding to Ru^0 and RuO_2, respectively [19]. Similarly, in Pt–Ru/MoC peaks at 461.94 and 463.58 eV correspond to Ru^0 and RuO_2, respectively. The peaks corresponding to Ru ($3p_{3/2}$) in Pt–Ru/WC at 461.99 and 464.53 eV, respectively, are for Ru^0 and RuO_2. It is noteworthy that Ru^0 is the predominant species in both Pt–Ru/MoC and Pt–Ru/WC catalysts. Unlike Pt which could be reduced from its oxides, Ru is not reduced under prevailing experimental conditions [20].

Figure 3(a) shows electro-catalytic activities for Pt–Ru/C, Pt–Ru/MoC, and Pt–Ru/WC towards methanol oxidation reaction (MOR). It is clear that both carbide-supported electro-catalysts show improved catalytic activity in relation to Pt–Ru/C. The load current-densities for MOR on carbide-supported catalysts are higher than the carbon-supported catalyst. Besides, the peak potentials for methanol-adsorbate oxidation for Pt–Ru/MoC, Pt–Ru/WC, and Pt–Ru/C are 0.54,
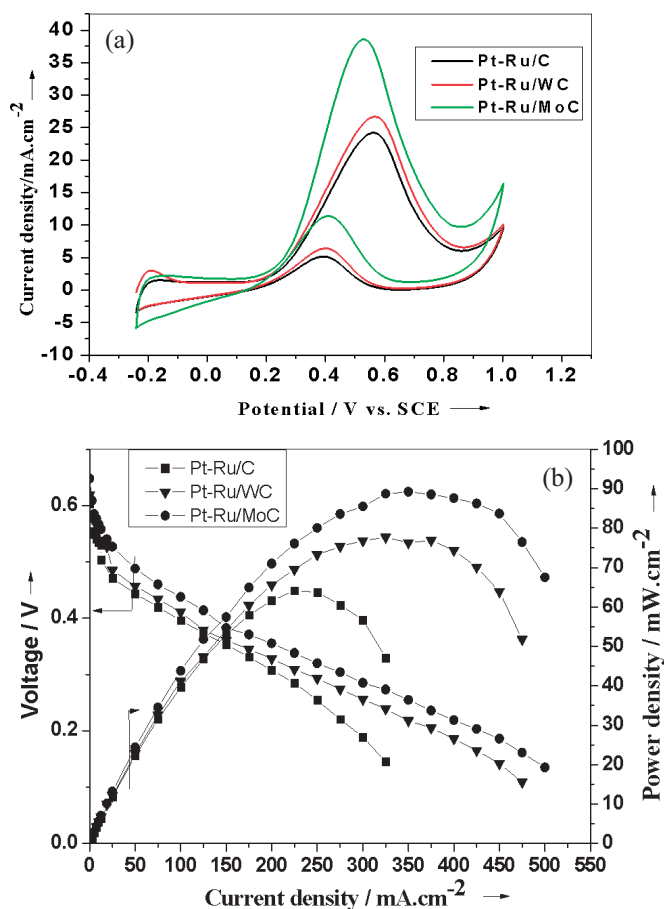
Fig. 3 (a) Cyclic voltammograms for methanol electro-oxidation for Pt–Ru/C, Pt–Ru/WC, and Pt–Ru/MoC in N_2-saturated aqueous solution containing aq. 0.5 M $HClO_4$ and aq. 0.5 M CH_3OH at a scan rate of 50 mV s^{-1} at 25 °C and (b) steady-state performance data for DMFCs with Pt–Ru/MoC, Pt–Ru/WC, and Pt–Ru/C anodes at 70 °C.

0.56, and 0.57 V, respectively, indicating that methanol oxidation occurs at a lower potential for carbide-supported catalysts in relation to carbon-supported catalyst. The enhanced catalytic activity may be due to a synergistic effect brought about by the interaction between Pt and metal carbide as it has been reported that carbide incorporation can enhance CO-tolerant activity for Pt. It can also be attributed to the weaker bonding between carbide and CO, which facilitates relatively easier desorption of CO from carbide surface [21]. Methanol oxidation activity is found to be in the following order: Pt–Ru/MoC > Pt–Ru/WC > Pt–Ru/C.

The catalysts have also been performance tested in DMFCs. The cell polarization data for DMFCs with Pt–Ru/MoC, Pt–Ru/WC, and Pt–Ru/C anodes are shown in Figure 3(b). It is clear that the DMFCs comprising carbide-supported anode catalysts are superior to Pt–Ru/C. The peak power-densities are 90, 78, and 65 mW cm^{-2} for Pt–Ru/MoC, Pt–Ru/WC, and Pt–Ru/C, respectively. These data are in conformity with CV data. Since cathode catalyst and the membrane electrolyte are kept identical during the study, the enhanced performance obtained for the DMFC with carbide-supported catalysts is a clear manifestation of the improved
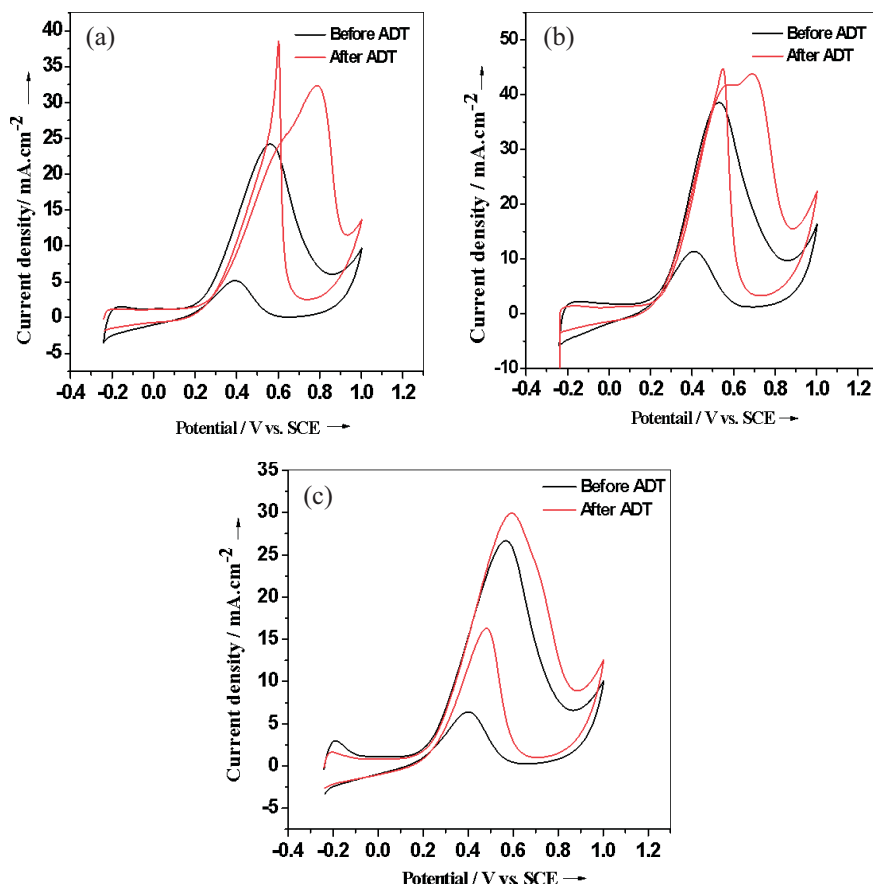
Fig. 4 Cyclic voltammograms for methanol electro-oxidation on (a) Pt–Ru/C, (b) Pt–Ru/MoC, and (c) Pt–Ru/WC electrodes in aq. 0.5 M CH$_3$OH and aq. 0.5 M HClO$_4$ before and after ADT at 25 °C.

methanol electro-oxidation behavior due to the carbide supports.

Figure 4 shows CV data for methanol oxidation before and after the durability test with Pt–Ru/C, Pt–Ru/MoC, and Pt–Ru/WC, respectively. It is seen that the methanol-adsorbate electro-oxidation peak shifts from 0.57 to 0.79 V after ADT for carbon-supported catalyst indicating decreased catalytic activity towards methanol oxidation after ADT. Furthermore, the positive onset potential shift and higher current after ADT suggest increase in platinum amount due to continuous Ru metal loss from Pt–Ru/C [22]. By contrast; carbide-supported electro-catalysts show much smaller shift in methanol-adsorbate and onset potentials after ADT. The data vividly suggest that carbide-supported catalysts are less affected by metal dissolution. This is corroborated by ICP-analysis where the concentration of Ru leached out from the catalysts is found to vary as: Pt–Ru/C (46 ppb) > Pt–Ru/MoC (14 ppb) > Pt–Ru/WC (10 ppb). These results confirm the higher stability of carbide supported Pt–Ru in relation to carbon-supported Pt–Ru towards methanol electro-oxidation reaction. This stability may be due to the excellent corrosion-tolerance of carbide in comparison to carbon black in acidic medium [23, 24]. The improved durability of carbide-supported electro-catalysts may also be due to the strong interac-

tion between Pt–Ru nanoparticles and carbide support. It is highly unlikely for Pt–Ru atoms on carbide support to agglomerate as larger particles to bring about a decrease in electrochemical activity or metal dissolution from the support surface [25].

4 Conclusion

Molybdenum carbide and WC are prepared and used as supports for Pt–Ru alloy catalyst. The enhanced catalytic activity and durability of Pt–Ru/MoC and Pt–Ru/WC catalysts in relation to Pt–Ru/C catalyst suggests that carbides are attractive alternative supports for Pt–Ru anode catalyst in DMFCs.

Acknowledgements

COMMUNICATION

References

[1] A. S. Aricò, V. Baglio, V. Antonucci, in *Electrocatalysis of Direct Methanol Fuel Cells* (Eds. H. Liu, J. Zhang), Wiley-VCH, Weinheim, **2009**.

[2] K. Scott, A. K. Shukla, *Direct Methanol Fuel Cell Fundamentals, Problems and Perspective* in *Modern Aspects of Electrochemistry* (Eds. R. E. White, C. G. Vayenas, M. A. Gamboa-Aldeco), Springer, New York, **2006**.

[3] L. Dubau, F. Hahn, C. Coutanceau, J. M. Leger, C. Lamy, *J. Electroanal. Chem.* **2003**, *554*, 407.

[4] J. F. Whitacre, T. Valdez, S. R. Narayanan, *J. Electrochem. Soc.* **2005**, *152*, A1780.

[5] P. Piela, C. Eicks, E. Brosha, F. Garzon, P. Zelenay, *J. Electrochem. Soc.* **2004**, *151*, A2053.

[6] E. H. Jung, U. H. Jung, T. H. Yang, D. H. Peak, D. H. Jung, S. H. Kim, *Int. J. Hydrogen Energy* **2007**, *32*, 903.

[7] T. M. Arruda, B. Shyam, J. S. Lawton, N. Ramaswamy, D. E. Budil, D. E. Ramaker, S. Mukerjee, *J. Phys. Chem. C* **2010**, *114*, 1028.

[8] Y. Chung, C. Pak, G. Park, W. S. Jeon, J. Kim, Y. Lee, H. Chang, D. Seung, *J. Phys. Chem. C* **2008**, *112*, 313.

[9] Y. Liu, C. Ji, W. Gu, J. Jorne, H. A. Gasteiger, *J. Electrochem. Soc.* **2011**, *158*, B614.

[10] H. H. Hwu, J. G. Chen, *Chem. Rev.* **2005**, *105*, 185.

[11] Z. Wang, P. Zuo, B. Liu, G. Yin, P. Shi, *Electrochem. Solid-state Lett.* **2009**, *12*, A13.

[12] D. J. Ham, J. S. Lee, *Energie* **2009**, *2*, 873.

[13] R. Ganesan, J. S. Lee, *Angew. Chem. Int. Ed.* **2005**, *44*, 6557.

[14] W. Liu, Y. Soneda, M. Kodama, J. Yamashita, H. Hatori, *Mater. Lett.* **2008**, *62*, 2766.

[15] T. Morishita, Y. Soneda, H. Hatori, M. Inagaki, *Electrochim. Acta* **2007**, *52*, 2478.

[16] K. G. Nishanth, P. Sridhar, S. Pitchumani, A. K. Shukla, *ECS Trans.* **2010**, *33*, 2027.

[17] G. Deganello, F. Giannici, A. Martorana, G. Pantaleo, A. Prestianni, A. Balerna, L. Liotta, A. Longo, *J. Phys. Chem. B* **2006**, *110*, 8731.

[18] C. Bock, C. Paquet, M. Couillard, G. A. Botton, B. R. MacDougall, *J. Am. Chem. Soc.* **2004**, *126*, 8028.

[19] J. Zhu, F. Cheng, Z. Tao, J. Chen, *J. Phys. Chem. C* **2008**, *112*, 6337.

[20] R. Chetty, W. Xia, S. Kundu, M. Bron, T. Reinecke, W. Schuhmann, M. Muhler, *Langmuir* **2009**, *25*, 3853.

[21] G. Lu, J. S. Cooper, P. J. McGinn, *J. Power Sources* **2006**, *161*, 106.

[22] Z. Jusys, J. Kaiser, R. J. Behm, *Electrochim. Acta* **2002**, *47*, 3693.

[23] Z. Y. Hu, M. Wu, Z. D. Wei, S. Q. Song, P. K. Shen, *J. Power Sources* **2007**, *166*, 458.

[24] H. H. Hwu, J. G. Chen, *J. Phy. Chem. B* **2003**, *107*, 2029.

[25] E. C. Weigert, A. L. Stottlemyr, M. B. Zellner, J. G. Chen, *J. Phy. Chem. B* **2007**, *111*, 14617.

_____